Performance Analysis of Open Steam Power Cycle Powered by Concentrated Solar Energy

Ayad Tareq Mustafa[*], Mohammed Mahmood Hadi

Department of Mechanical, College of Engineering, Al-Nahrain University, Baghdad, Iraq

Abstract

This study aims to develop a concentrated solar receiver designed to directly generate steam for driving a steam turbine within the steam power cycle of a carbon-free system. The solar power system consists of parabolic dishes, evaporation tanks, and a steam turbine, and the experimental setup was tested on different days, analyzing the measured parameters with the EES software. Results from the investigation indicate that, under the optimal conditions with a maximum recorded temperature and pressure of 143 ℃ and 2.5 bar, respectively, and a vaporized water mass of 100 grams, the manufactured turbine achieved a maximum isentropic efficiency of 92.48% and a power of 1.76 W. Notably, the evaporation tank and the mini steam turbine demonstrated the capability to generate steam and mechanical power, respectively, without relying on conventional energy.

Keywords: parabolic dish collector, steam turbine, solar energy, performance analysis, power generation

1. Introduction

The energy gained from the sun is the basis for other forms of energy sources in the world such as oil, natural gas, and coal, this is attributed to the process of photosynthesis in plants. The complex chemical reactions within photosynthesis produce the energy that ultimately becomes the basis for other energy sources. To exploit the free solar energy and convert it into efficient energy in daily lives, different solar-thermal power cycles had been developed [1-2].

The Rankine steam cycle, shown in Fig. 1, involves heating water passing through the boiler to generate superheated steam; and then pressurized steam is fed into an expander called a turbine. The steam cycle utilizes concentrated solar thermal (CST) technology as a heat source; the water is converted to pressurized steam to spin a turbine [2-3]. Solar thermal power plants generally generate steam at pressures ranging between 60-100 bars. The turbine efficiency of heat/electricity is commonly in the range of 35-38%, which needs high temperatures to raise the conversion efficiency [4].

One of the promised CST types is parabolic trough solar collectors that are used to generate electrical power. The parabolic trough collectors can be applied on small and large scale, such as for a residence and a power plant, respectively [5]. Heat transfer enhancement in CST collectors is a crucial point. The investigation of nanofluids as working thermo-fluid shows an increase in heat transfer coefficient by 21% when using nanofluids of $TiO_2 + Cu$ hybrid in the parabolic trough collectors [6].

Steam generation in the Rankine cycle, in addition to solar-assisted steam generation, was presented in previous studies. Sakhare and Kapatkar [7] obtained the best findings with a 170 ℃ outlet temperature at a 90 ℃ inlet temperature from a coiled pipe receiver. This occurred under an average solar radiation of 714 W/m^2. Additionally, Arulkumaran and Christraj [8] recorded an outlet temperature of 190 ℃ for a water flow rate of 0.35 kg/s with solar radiation of 490 W/m^2, achieved through 24 turns of the copper-coiled tube.

---

* Corresponding author. E-mail address: ayad_altai@yahoo.com

Also, Folaranmi [9] recorded a measurement of an exit temperature of 200 ℃ by the heat exchanger for 1 kg of charged water, and Aljabair et al. [10] measured an outlet temperature of 126 ℃ using a heat exchanger receiver of dimensions (47 cm × 37 cm) with corrugated fins. Moreover, Sada and Sa'ad-Aldeen [11] obtained the outlet temperature of 118 ℃ from the thermal receiver with a copper coiled tube of dimension (1.25 cm × 300 cm). On the other hand, Escobar-Romero et al. [12] utilized the parabolic trough reflector to generate the steam at high pressure and temperature that reached 6.6 bar and 155 ℃, respectively.
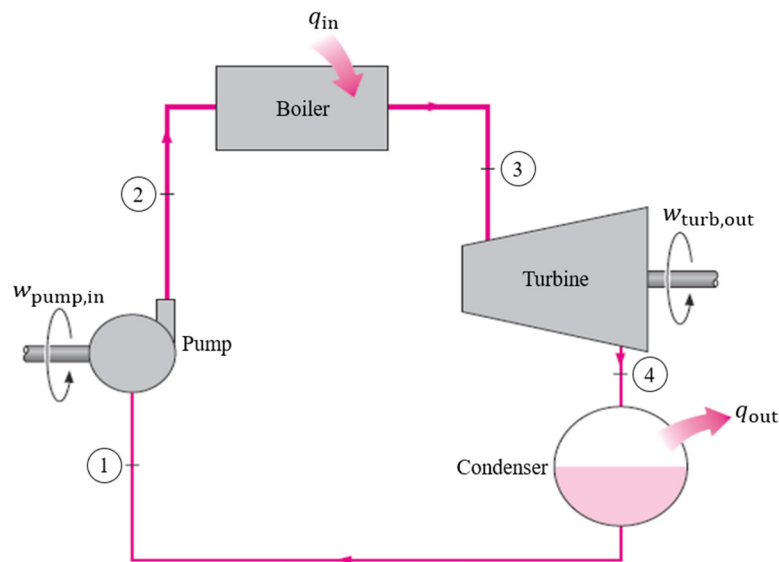

Fig. 1 Simple Rankine steam cycle [13]

Several studies have been achieved on power generation systems that utilize solar thermal energy with the organic Rankine cycle (ORC) under different operating conditions. A concentric parabolic trough as a steam generator was designed by Mohammad et al. [14] to theoretically study the steam power plant with a maximum temperature of 350 ℃, operating pressure of 5.2 bar, and 57% optical efficiency. ORC with direct evaporation in coiled tubing was designed, which exchanges heat with the exhaust gas flow in the shell side [15].

It is revealed that the maximum heat of 225 kW in the direct evaporator has been achieved. Also, Linnemann et al. [16] tested a dual consecutive ORC using different working fuels to get a maximum generation power of 17.5 kW from the power plant. Moreover, a low-pressure ORC with a steam turbine and double heat exchangers was designed and tested, in which the maximum power generated is 302 kW when the thermal efficiency is 9.7% [17]. Achieving a power generation of 1.17 MW and a solar-to-electricity efficiency of 21.59%, the hybrid plant integrates a capacity of 500 tons/day for incinerated waste materials with a solar thermal power collector [18].

Gao et al. [19] proposed a power generation system utilizing ORC with solar thermal accumulators. Gao et al. [20] proposed a developed power generation system using solar thermal energy with a mixing room, in which the mixing room temperature has an important role in the thermal efficiency of the system. Maytorena and Buentello-Montoya [21] simulated the ORC integrated with a parabolic trough collector to generate power using Ansys-Fluent software. The results demonstrated that the fluid evaporation rate increases when the mass flow rate decreases, and the evaporation rate of the fluid is directly proportional to the solar radiation increase. Loni et al. [22] reviewed the power generation technology by solar irradiation driving the ORCs based on the compatibility between the temperature produced by the solar collector and the temperature required for the ORC to work.

A real challenge to the steam power cycle using solar radiation was inferred, due to the low temperatures of the water produced by the tested receivers of the parabolic dish, except for the evaporation tank [23]. On the other hand, previous studies revealed that solar collectors are used to support the working fluid in the Rankine cycle by increasing the steam temperature

before entering the steam turbine. Therefore, developing a concentrated solar receiver to generate steam directly to spin the steam turbine in a carbon-free system lacks examination and evaluation. The current study aims to investigate the performance of an open steam power cycle built of parabolic solar collectors with a mini steam turbine and to thermally analyze the new steam power system.

2. Experimental Work

The research objectives can be achieved through the implemented methodology. The experimental test rig is made up of solar parabolic dish reflectors, receivers for reflected radiation, and a mini steam turbine. The materials, dimensions, and fabrication process have been described. The measuring instruments, experiment procedures, and error analysis have also been demonstrated.

2.1. *Experimental setup*

Two parabolic dishes are used to reflect incident solar radiation and heat the steam generation receivers. The parabolic dish reflectors are constructed with an adjustable structure to allow the sun to follow up vertically. The face of each dish is constructed from small square pieces of the mirror of 3 cm in length and reflectivity of 0.9.

In the present work, three types of receivers were fabricated and tested. The helical coil and cylindrical cavity were modeled experimentally and tested in the first stage of the current research. Then, the evaporation tank receiver was implemented successfully to generate water vapor. The investigation of the three receivers shows that the efficiency and steam-generated rate of the evaporation tank receiver is greater than the other two types [23]. Therefore in the present study, the evaporation tank receivers have been used at the focal point of the parabolic dish reflectors, which appear to be reliable receivers for generating steam. Each receiver tank is made of a 1.6 mm thick metallic brass plate. The evaporation tank is made of parallelepiped plates, 7 cm in deep with a square face of (10×10) cm^2 that is designed to be compatible with the area of reflected radiation, as shown in Fig. 2. The heat absorbed from the tank front plate is transfer to vaporize water inside. The fabricated evaporation tanks were tested under the operational limitations of the water mass and vaporization time.
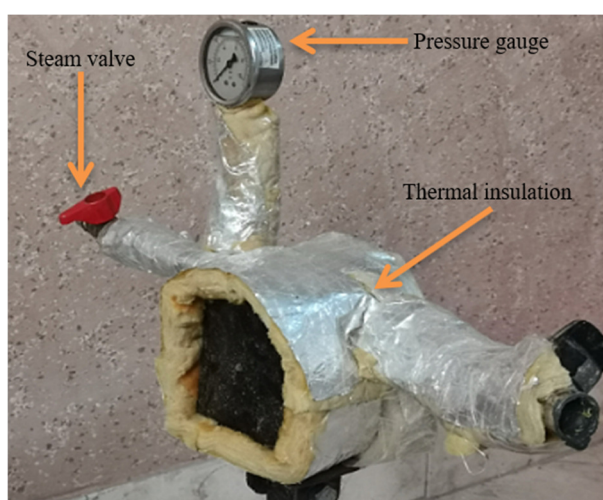

Fig. 2 Pictorial of evaporation tank

The third part of the experimental setup is a mini steam turbine, which was made with a diameter of 12 mm stainless steel centrifugal blades. The centrifugal turbine includes the rotor, cylindrical cover, two flange cubs, two mini ball bearings, and the rotor shaft, as shown in Fig. 3. The cylindrical cover and two sides flange cub were made of brass. The cylindrical cover included two holes of 6 mm in diameter for inlet and outlet copper tubes allowing working fluid to flow. The inlet steam flow affects tangentially the rotor blades to spin the turbine. The components of the current test rig are summarized in Table 1 through the material used, dimensions, quantity, also parameters tested.
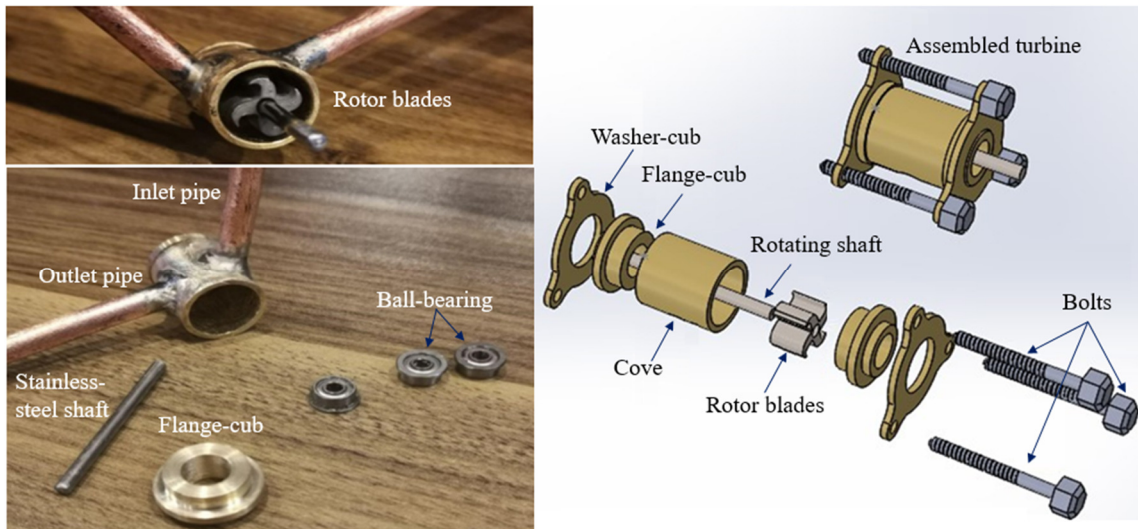
Fig. 3 Schematic and photographs of mini steam turbine parts and dimensions

Table 1 Experimental test rig summarization

The component	Manufacturing				Test parameters
	Item	Material	Dimensions	Quantity	
Parabolic dishes	Dish	Steel	D1 = 83 cm D2 = 74 cm	2	Incident solar radiation
	Mirrors	Glass	(3×3) cm^2	960	
Solar radiation receivers	Evaporation tank	Brass plate - 1.6 mm thickness	$(10 \times 10 \times 7)$ cm^3	2	Temperature and pressure of generated steam
Mini steam turbine	Rotor blades	Stainless steel	ϕ_{outer} = 12 mm	1	Temperature and pressure of inlet and outlet steam
	Cylindrical cover	Brass	ϕ_{inner} = 14 mm ϕ_{outer} = 17 mm	1	
	Flanges	Brass	ϕ_{outer} = 18 mm	2	
	Rotor shaft	Stainless steel	ϕ_{outer} = 3 mm	1	
	Ball bearings	Stainless steel	ϕ_{outer} = 8 mm	2	

2.2. Measuring instruments

Various parameters such as solar intensity, temperature and pressure of steam generated, and vapor flow rate were measured using different measuring instruments. The solar meter is used for measuring the solar radiation falling directly on the parabolic dish during daily test hours. Thermocouples and thermometers type-K have been used to measure the temperature of the surfaces of the pipes carrying the working fluid. Also, pressure gauges ranging between 0 to 10 bars were used to measure the vapor pressure generated in the present solar power system. The vapor flow rate was measured using the orifice plate flow meter. The operational principle is based on the fluid passed through a pipeline restriction, and the differential pressure is measured through this restriction. The orifice plate was designed and fabricated in the present work, as shown in Fig. 4.
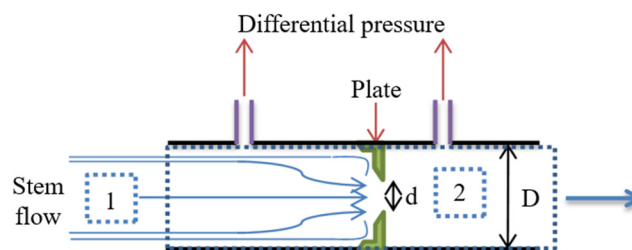

Fig. 4 Diagram of the orifice plate

2.3. Experimental procedure of power system with double collectors

The current system is constructed from two parabolic dish reflectors with two evaporation tank receivers, as shown in Fig. 5. The first evaporation tank is used as the main steam generator for each hour of testing and then the generated steam flows through the second evaporation tank to augment more heating and improve its thermal characteristics. The generated vapor passed through the orifice flow meter and then the steam turbine to measure the steam mass flow rate and produce the mechanical power, respectively. The test of the current system was conducted from June to July 2021 in Al-Fallujah, Iraq (33.16°N, 43.87°E) accordance with the following steps:

(1) The power system setup is prepared at 8 am by orienting the collector towards the sun manually and at the beginning of each hour of the test; the measurements are recorded from 9 am to 3 pm.

(2) The evaporation tank is injected with a mass of water weighing 100 grams every hour of the test, while the inlet valve is closed.

(3) The outlet valves of the evaporation tanks are closed at first. The valve between the first and second evaporation tanks is opened after 30 minutes of the tested hour. After 20 minutes, the exit valve next to the second evaporation tank is opened to allow the generated steam to flow through the orifice plate and steam turbine.

(4) Several parameters were measured at each tested hour, the average solar radiation falling on the two dishes, the temperature at the four points shown, and the pressure at the five points shown in the solar power system schematic.

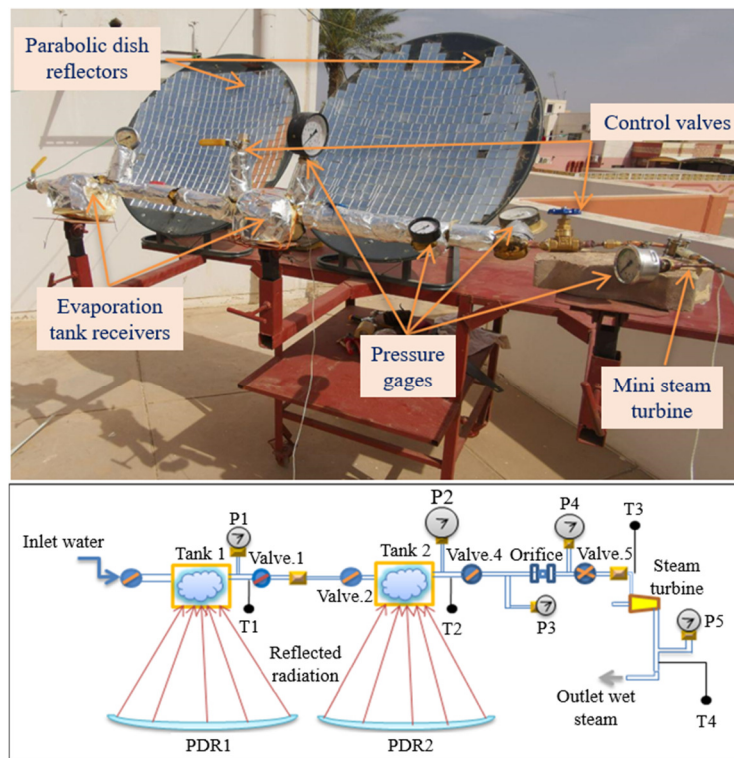(5) The above procedure has been repeated for the masses of water of (150, 200, 250, and 300) grams on different days.

Fig. 5 Photograph and schematic of solar power system with double collectors

2.4. Thermal analysis

The measured parameters have been used to analyze the power system thermally. The heat absorbed by the evaporation tank and the power produced by the steam turbine is mainly equal to the change in the specific enthalpy of the working fluid. To estimate the solar radiation received by the evaporation tank, reflected radiation from the solar collector can be calculated as follows [24]:

$$I_r = I_T \times A_a \times r \tag{1}$$

where I_r is the reflected solar radiation (W), I_T is the total incident solar radiation (W/m^2), A_a is the aperture area (m^2), and r is the mirror reflectivity.

The useful heat rate absorbed by the evaporation tanks of the double collector power system can be calculated according to the following equation [13]:

$$Q_u = m_s \times (h_1 - h_i) \tag{2}$$

where h_i is the specific enthalpy (kJ/kg) of inlet water at a temperature of 25 °C, h_1 is the specific enthalpy of steam leaving the evaporator (kJ/kg), and m_s is the mass flow rate of steam (kg/s).

The steam, after leaving the evaporation tanks, passes through the orifice plate toward the steam turbine. The power produced by the mini steam turbine can calculated as follows [25]:

$$W_T = m_s \times (h_2 - h_3) \tag{3}$$

where h_2 is the specific enthalpy of steam entering the turbine (kJ/kg) and h_3 is the specific enthalpy of steam leaving the turbine (kJ/kg).

The performance of the steam turbine is assessed by obtaining the isentropic efficiency of the mini steam turbine, as described in the formula below. The isentropic efficiency indicates the ratio of the actual expansion to the isentropic expansion of the steam. The work of actual expansion is less than the work of isentropic expansion [13].

$$\eta_T = \frac{h_2 - h_3}{h_2 - h_{3s}} \tag{4}$$

The thermal efficiency of the present power system can evaluated by dividing the work of the steam turbine by the useful heat rate absorbed by the evaporation tanks. The thermal processes of the present power system were implemented and analyzed through an open steam cycle using the EES software.

2.5. Errors analysis

Most of the standard errors have mainly been caused by errors in the measured quantities due to the accuracy of the measuring devices. To determine the uncertainty in the evaporation efficiency value that represents the useful heat rate absorbed relative to the total incident solar radiation. The amount of error resulting from the error of measuring the pressure and temperature of the steam has been determined by finding the amount of change in the specific enthalpy difference and its effect on the efficiency of the evaporation. The uncertainty intervals, w, in the results, were calculated by using the following equation:

$$W_R / R = \left[(\partial R / \partial v_1 \times w_1 / R) \wedge 2 + (\partial R / \partial v_2 \times w_2 / R) \wedge 2 + \ldots + (\partial R / \partial v_n \times w_n / R) \wedge 2 \right] \wedge 0.5 \tag{5}$$

The accuracy range of the measuring instruments used is shown in Table 2. For total incident, solar radiation of 716.6 W/m^2, the pressure, and temperature of generated steam are 3 bar and 140.7 °C, respectively. The specific enthalpy difference of generated steam is 2.65×10^3 kJ/kg, and the evaporation efficiency is 19%. Subsequently, the predicted uncertainty of the evaporation efficiency is 0.0145, which indicates an acceptable value.

Table 2 Uncertainties in measuring instruments

Independent variables	Accuracy interval
Pressure gauge	±0.05 bar
Temperature	±0.1 °C
Incident radiation	±10 W/m^2

3. Results and Discussion

Experimental results and thermal analysis of the double collectors' power system were illustrated and discussed with clear interpretations. The change in the thermal properties of the generated steam over time is due to the change in solar thermal radiation. On the other side, the thermodynamic processes of steam generated in the current power system were discussed.

3.1. Experimental results

The parameters measured in the current study rely on the solar radiation received. The measured solar radiation intensity varied during the test time, for instance, from 585 W/m² at 9 am to 704 W/m² at 3 pm on Joly 15, 2021, for 250 grams of tested water.

3.1.1. Temperature of generated steam

The temperature of the generated steam is measured before the steam enters the turbine to study the effects of the temperature change on the properties of the steam. The results demonstrate increasing steam temperature when the time increases from 9:00 am to the peak value at 1:00 pm, and then the temperature decreases. Also, the outcomes show a decrease in the steam temperature when the mass of tested water increases from 100 to 300 grams.

The vapor temperatures measured within the double collectors' power system shown in Fig. 5 are T1, T2, T3, and T4. Fig. 6 shows the temperature variation within the double collectors at 1:00 pm and the evaporating mass of 200 grams. The temperatures T1 and T2 represent the temperatures of the steam leaving the first and second steam generators, respectively. The temperatures T3, T4, and Ta represent the temperature of steam entering the turbine, the temperature of steam leaving the turbine, and ambient temperature, respectively. The temperature difference between T1 and T2 dates back to the steam expansion when the exit valve of the first steam generator opened. The temperature difference between T2 and T3 indicates the thermal loss to the surroundings and pressure drop within the orifice plate. While the temperature difference between T3 and T4 represents the heat utilized in the steam turbine. The high temperatures of T1, T2, and T3 give preference to the double collectors than the single one in producing the power.
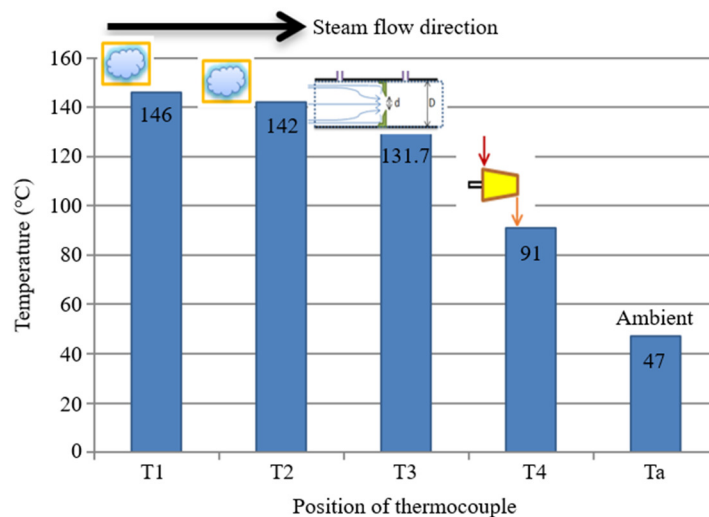

Fig. 6 Comparison of temperatures within the power system at 1:00 PM and
200 g of tested water (18/7/2021)

3.1.2. Mass flow rate of generated steam

The mass flow rate of generated steam through test time is a function of the differential pressure across the orifice plate. Due to the direct proportionality between the vapor flow rate and the differential pressure, the velocity of the steam generated across the orifice plate area can estimated, which means that the mass flow rate of the generated vapor is determined. The mass

flow rate variation, for instance, for 100 grams of tested water shown in Fig. 7, the mass flow rate increases from 0.0164 g/s at 9:00 to 0.018 g/s at 1:00, and then it decreases to 0.0174 g/s. The variance in the vapor flow rate is due to the mass of the tested water and the heat absorbed by the tank during daylight hours. Fig. 7 shows the increasing mass flow rate of generated steam, generally, when the masses of tested water decrease due to current testing limitations in evaporation tank receiver size and incident solar radiation. This behavior is consistent with the results obtained by Maytorena and Buentello-Montoya [21] in increasing the evaporation rate when the mass rate decreases.
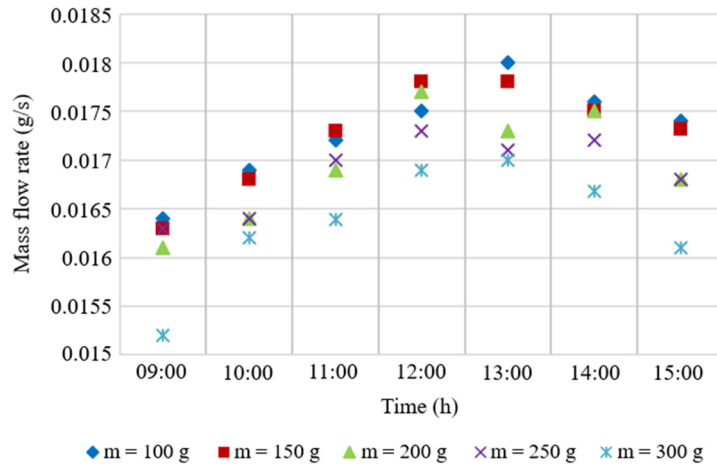

Fig 7 Distribution of mass flow rate of generated steam versus time for different masses of tested water

3.2. Thermal analysis

The performance of the current power system has been verified based on the measured parameters affected by the solar radiation namely steam temperature and pressure, and the mass flow rate of the generated steam. The power system performance has been realized through the useful heat of the evaporator, power production and efficiency of the steam turbine, and thermodynamic processes.

3.2.1. Useful heat rate absorbed by evaporation tank
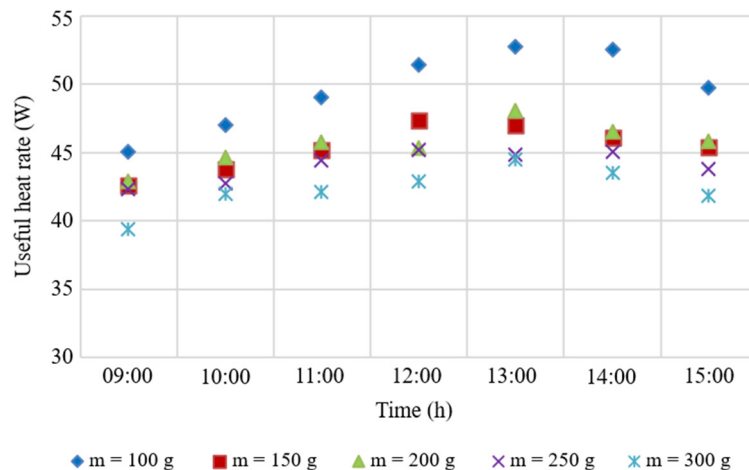

Fig. 8 Distribution of evaporator useful heat rate versus time for different masses of tested water

The useful heat of the evaporator is an important parameter that refers to the heat absorbed by the water in the evaporation tank from the reflected irradiance. Fig. 8 shows the distribution of the evaporator's useful heat rate versus time, which is evaluated by Eq. (2). The figure shows the increasing useful heat rate absorbed by the two evaporators when time increases toward 1 pm then it decreases. While the absorbed useful heat rate decreases when the mass of tested water increases. The

reason is due to the change in the rate of steam production over time, where when the rate of steam generation shown in Fig. 7 rises, the useful heat rate increases at a finite time, and vice versa. It has been discovered that the heat rate of the double collectors is higher than that of a single collector when assessed at the same time and with the same amount of water. Adding a second evaporation tank helps to increase the energy used to evaporate the water being tested. This results in higher thermal properties for the steam that is generated during testing.

3.2.2. Steam turbine power production

The power produced by the mini steam turbine could be described as the specific enthalpy difference in the steam flows through the rotor blades, as stated in Eq. (3). Fig. 9 shows the distribution of power produced by the mini steam turbine versus time for different masses of tested water. The figure reveals a decrease in the power of the steam turbine when the masses of tested water increase due to the small size of the steam turbine used. The maximum power produced by the steam turbine for the tested masses of evaporating water (100, 150, 200, 250, and 300) grams are (1.76, 1.62, 1.66, 1.20, and 1.06) watts, respectively. The maximum power of the manufactured turbine is 1.76 W for the maximum recorded temperature and pressure of generated steam at 143 °C and 2.5 bar and vaporized water of 100 grams. The power produced by the steam passage through the rotor blades provides the energy to produce mechanical power. The current outcomes found that the mini turbine is more powerful and practical when used with double collectors compared to a single collector in the proposed steam power system due to the increment in the power produced.
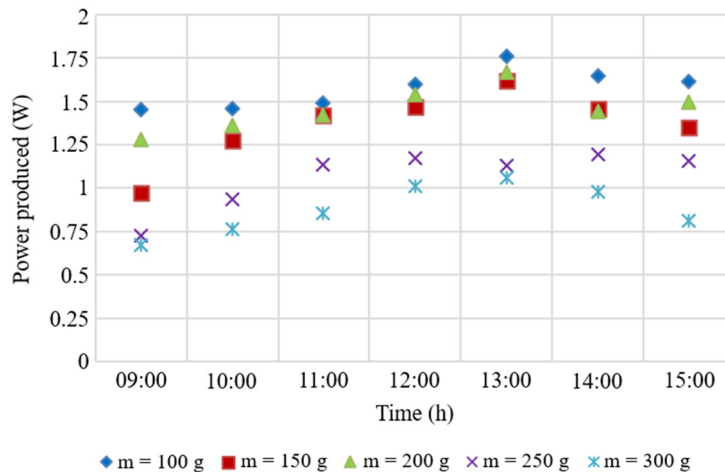

Fig. 9 Distribution of power produced by the mini steam turbine versus time
for different masses of tested water

3.2.3. Performance of steam turbine

The operational performance of the mini steam turbine manufactured in the current study can evaluated by combining the parameters of steam turbine efficiency and power produced by the turbine when the mass flow rate of generated steam changes through the power system. The combination of turbine efficiency, power produced, and mass flow rate of steam to verify the performance of the mini steam turbine was analyzed experimentally for the first time under the effect of pure green energy. Fig. 10 shows the performance of the steam turbine used in the double solar collectors' power system for the mass of tested water of 150 grams. Based on real-time changes, the figure illustrates how the efficiency and power output of the turbine vary with fluctuations in steam mass flow rate. The x-axis displays the corresponding values.

Curves of the polynomial trend for the data shown in Fig. 10 were carried out with R-squared values of 0.96 and 0.99 for data of power produced and the isentropic efficiency, respectively. The best point of operation for the mini steam turbine used in the current power system has been stated by the point of intersection between the two curves, which matches the values of 0.0169 g/s steam mass flow rate, 1.31 W power produced, and 71.4% turbine efficiency, as shown in Fig. 10. The recorded

solar radiation, corresponding to the best steam flow rate of the current turbine, is approximately 626 W/m². Based on the behaviors observed and the operating point obtained, it is in line with the typical trend of steam turbine operation, whilst no prior data is available.
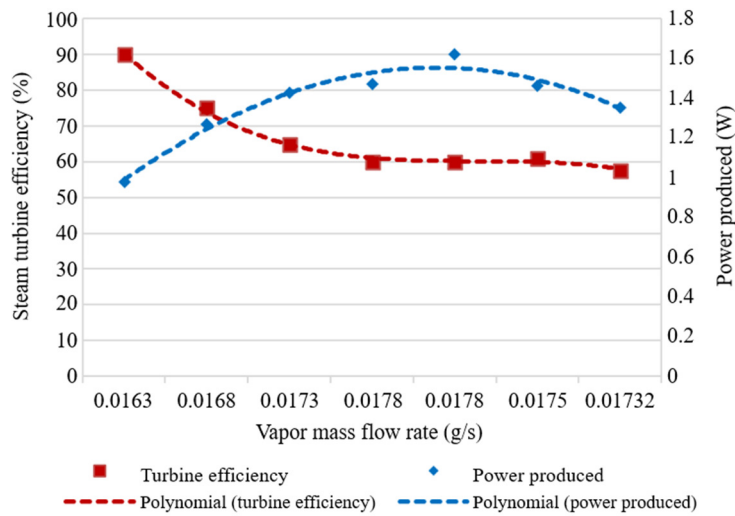

Fig. 10 Performance of the mini steam turbine for the mass of tested water 150 g
(12/7/2021)

3.3. Thermodynamic processes

Water was used as a working fluid in the present power system, where the water vapor generated in the evaporation tanks is forced through the orifice plate tube towards the steam turbine to generate the mechanical power in an open steam cycle. The behavior of the working fluid was analyzed by representing the thermodynamic process of the current cycle on a T-s diagram of the water vapor properties using an engineering equation solver, EES.

Three thermal processes of 300 grams of evaporated water at different hours of 9:00 am, 1:00 pm, and 3:00 pm are shown in Fig. 11. The process of steam generation within the two evaporation tanks was considered one thermal process to generate superheated steam. The lines [1-2], [1-2°], and [1-$\overline{2}$] shown in Fig. 11 represent the evaporation process, the lines [2-3], [2°-3°], and [$\overline{2}$-$\overline{3}$] represent the steam passes through the orifice tube, and the lines [3-4], [3°-4°], and [$\overline{3}$-$\overline{4}$] represent the steam expansion process through the turbine. The figure reveals that the thermodynamic properties of steam generated and the power production at 1:00 pm are higher than those at 3:00 pm and 9:00 am. Also, it can concluded that the steam generation and the power of the turbine increase when the evaporated mass in the tank decreases.
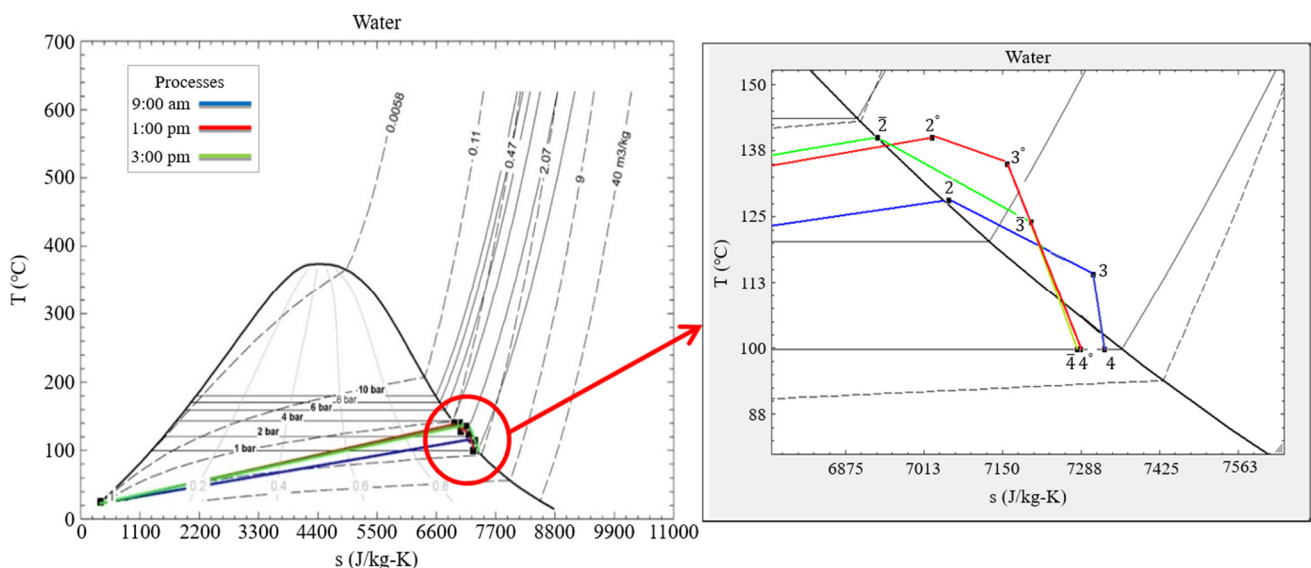

Fig. 11 Thermal processes of generated steam for an evaporated water mass of 300 g and different times

4. Conclusions

In this study, the thermal solar power system has been fabricated and tested to produce steam with suitable thermal properties for driving the steam turbine, serving as a first stage in power generation. The conclusions drawn from the current outcomes and discussions are elaborated as follows:

(1) The evaporation tank and the mini steam turbine are capable of generating steam and mechanical power, respectively. These can be utilized in developing a large-scale power system, especially when incorporated into a closed-cycle power system.

(2) The useful heat rate, power produced, and efficiency of the steam turbine increase when the masses of tested water decrease. This effect is attributed to the limitation of the absorbed irradiance relative to the limited volume of the evaporation tanks.

(3) At the maximum recorded temperature of 143 °C and pressure of generated steam of 2.5 bar, with a vaporized water mass of 100 grams, the steam turbine achieves maximum isentropic efficiency and power of 92.48% and 1.76 W, respectively.

(4) The best point of operation for the mini steam turbine in the current power system is identified at the mass flow rate of steam of 0.0169 g/s, resulting in 1.31 W of power produced, a turbine efficiency of 71.4%, and incident solar radiation of 626 W/m^2.

(5) The turbine power produced and the useful heat rate with double collectors surpass those of using a single collector system for the same amount of water tested, making it a more practical option.

The global aspirations for a carbon-free power generation system, achieved by harnessing solar radiation to power the Rankine steam cycle, can be realized through the development of the solar steam power system investigated in this study. The intention is to operate it within a closed steam cycle, a concept planned to be verified in the second stage of power generation.

Conflicts of Interest

The authors declare no conflict of interest.

References

[1] J. A. Duffie and W. A. Beckman, Solar Engineering of Thermal Processes, 4th ed., Hoboken: John Wiley, 2013.

[2] M. Blanco and L. R. Santigosa, Advances in Concentrating Solar Thermal Research and Technology, Duxford: Woodhead Publishing is an imprint of Elsevier, 2017.

[3] C. Christopher Newton, "A Concentrated Solar Thermal Energy System," MSc. thesis, Department of Mechanical Engineering, Florida State University, Tallahassee, FL, 2007.

[4] M. Livshits and A. Kribus, "Solar Hybrid Steam Injection Gas Turbine (STIG) Cycle," Solar Energy, vol. 86, no. 1, pp. 190-199, January 2012.

[5] A. Ahmad, O. Prakash, R. Kausher, G. Kumar, S. Pandey, and S. M. M. Hasnain, "Parabolic Trough Solar Collectors: A Sustainable and Efficient Energy Source," Materials Science for Energy Technologies, vol. 7, pp. 99-106, 2024.

[6] L. A. Omeiza, M. Abid, Y. Subramanian, A. Dhanasekaran, S. A. Bakar, and A. K. Azad, "Challenges, Limitations, and Applications of Nanofluids in Solar Thermal Collectors—A Comprehensive Review," Environmental Science and Pollution Research, in press. https://doi.org/10.1007/s11356-023-30656-9

[7] V. Sakhare and V. N. Kapatkar, "Experimental Analysis of Parabolic Solar Dish with Copper Helical Coil Receiver," International Journal of Innovative Research in Advanced Engineering, vol. 1, no. 8, pp. 199-204, September 2014.

[8] M. Arulkumaran and W. Christraj, "Experimental Analysis of Non-Tracking Solar Parabolic Dish Concentrating System for Steam Generation," Engineering Journal, vol. 16, no. 2, pp. 53-60, February 2012.

[9] J. Folaranmi, "Design, Construction and Testing of a Parabolic Solar Steam Generator," Leonardo Electronic Journal of Practices and Technologies, vol. 8, no. 14, pp. 115-133, January-June 2009.

[10] S. Aljabair, L. J. Habeeb, and A. M. Ali, "Experimental Analysis of Parabolic Solar Dish with Radiator Heat Exchanger Receiver," Journal of Engineering Science and Technology, vol. 15, no. 1, pp. 437-454, February 2020.

[11] G. K. A. Sada and A. E. Sa'ad-Aldeen, "Experimental Steady to Produce Steam by Solar Energy Using Solar Dish Concentration with Copper Coil Receiver," International Journal of Engineering and Innovative Technology, vol. 4, no. 7, pp. 147-149, January 2015.

[12] J. F. M. Escobar-Romero, S. V. Y. y Montiel, F. Granados-Agustín, V. M. Cruz-Martínez, E. Rodríguez-Rivera, and L. Martínez-Yáñez, "Building a Parabolic Solar Concentrator Prototype," Journal of Physics: Conference Series, vol. 274, article no. 012104, 2011.

[13] Y. A. Cengel, M. A. Boles, and M. Kanoglu, Thermodynamics: An Engineering Approach, vol. 5, New York: McGraw-Hill, 2011.

[14] S. T. Mohammad, H. H. Al-Kayiem, and M. K. Assadi, "Developed Mathematical Model of Solar Thermal Parabolic Trough Power Plant at Universiti Teknologi Petronas," ARPN Journal of Engineering and Applied Sciences, vol. 11, no. 20, pp. 12140-12145, October 2016.

[15] M. Linnemann, K. P. Priebe, G. Herres, C. Wolff, and J. Vrabec, "Design and Test of a Multi-Coil Helical Evaporator for a High Temperature Organic Rankine Cycle Plant Driven by Biogas Waste Heat," Energy Conversion and Management, vol. 195, pp. 1402-1414, September 2019.

[16] M. Linnemann, K. P. Priebe, A. Heim, C. Wolff, and J. Vrabec, "Experimental Investigation of a Cascaded Organic Rankine Cycle Plant for the Utilization of Waste Heat at High and Low Temperature Levels," Energy Conversion and Management, vol. 205, article no. 112381, February 2020.

[17] D. Wang, X. Dai, Z. Wu, W. Zhao, P. Wang, B. Hu, et al., "Design and Testing of a 340 kW Organic Rankine Cycle System for Low Pressure Saturated Steam Heat Source," Energy, vol. 210, article no. 118380, November 2020.

[18] H. Chen, Y. Wu, Y. Zeng, G. Xu, and W. Liu, "Performance Analysis of a Solar-Aided Waste-to-Energy System Based on Steam Reheating," Applied Thermal Engineering, vol. 185, article no. 116445, February 2021.

[19] G. Gao, J. Li, P. Li, J. Cao, G. Pei, Y. N. Dabwan, et al., "Design of Steam Condensation Temperature for an Innovative Solar Thermal Power Generation System Using Cascade Rankine Cycle and Two-Stage Accumulators," Energy Conversion and Management, vol. 184, pp. 389-401, March 2019.

[20] G. Gao, J. Li, P. Li, H. Yang, G. Pei, and J. Ji, "Design and Analysis of an Innovative Concentrated Solar Power System Using Cascade Organic Rankine Cycle and Two-Tank Water/Steam Storage," Energy Conversion and Management, vol. 237, article no. 114108, June 2021.

[21] V. M. Maytorena and D. A. Buentello-Montoya, "Multiphase Simulation and Parametric Study of Direct Vapor Generation for a Solar Organic Rankine Cycle," Applied Thermal Engineering, vol. 216, article no. 119096, November 2022.

[22] R. Loni, O. Mahian, C. N. Markides, E. Bellos, W. G. Le Roux, A. Kasaeian, et al., "A Review of Solar-Driven Organic Rankine Cycles: Recent Challenges and Future Outlook," Renewable and Sustainable Energy Reviews, vol. 150, article no. 111410, October 2021.

[23] A. T. Mustafa and M. M. Hadi, "A Comparative Study of Multi-Form Steam Generators Using Concentrated Solar Power," Journal of Advanced Research in Fluid Mechanics and Thermal Sciences, vol. 88, no. 2, pp. 157-168, December 2021.

[24] R. K. M. Al Dulaimi, "Experimental Investigation of the Receiver of a Solar Thermal Dish Collector with a Dual Layer, Staggered Tube Arrangement, and Multiscale Diameter," Energy Exploration & Exploitation, vol. 38, no. 4, pp. 1212-1227, July 2020.

[25] S. L. Dixon and C. Hall, Fluid Mechanics and Thermodynamics of Turbomachinery, 7th ed., Oxford: Butterworth-Heinemann, 2014.